Vaccine 33 (2015) 1360–1368

Contents lists available at ScienceDirect

Vaccine

journal homepage: www.elsevier.com/locate/vaccine

Site-specific characterization of envelope protein N-glycosylation on Sanofi Pasteur's tetravalent CYD dengue vaccine

Jean Dubayle*, Sandrine Vialle, Diane Schneider, Jérémy Pontvianne, Nathalie Mantel, Olivier Adam, Bruno Guy, Philippe Talaga

Research and Development Department, Sanofi Pasteur, Campus Mérieux, 1541 Avenue Marcel Mérieux, 69280 Marcy L'Etoile, France

ARTICLE INFO

Article history:
Received 3 November 2014
Received in revised form 9 January 2015
Accepted 11 January 2015
Available online 3 February 2015

Keywords:
Dengue virus
Envelope protein
Mass spectrometry
N-glycosylation

ABSTRACT

Recently, several virus studies have shown that protein glycosylation play a fundamental role in the virus–host cell interaction. Glycosylation characterization of the envelope proteins in both insect and mammalian cell-derived dengue virus (DENV) has established that two potential glycosylation residues, the asparagine 67 and 153 can potentially be glycosylated. Moreover, it appears that the glycosylation of these two residues can influence dramatically the virus production and the infection spreading in either mosquito or mammalian cells.

The Sanofi Pasteur tetravalent dengue vaccine (CYD) consists of four chimeric viruses produced in mammalian vero cells. As DENV, the CYDs are able to infect human monocyte-derived dendritic cells *in vitro via* C-type lectins cell-surface molecules. Despite the importance of this interaction, the specific glycosylation pattern of the DENV has not been clearly documented so far. In this paper, we investigated the structure of the N-linked glycans in the four CYD serotypes.

Using MALDI-TOF analysis, the N-linked glycans of CYDs were found to be a mix of high-mannose, hybrid and complex glycans. Site-specific N-glycosylation analysis of CYDs using nanoLC–ESI-MS/MS demonstrates that both asparagine residues 67 and 153 are glycosylated. Predominant glycoforms at asparagine 67 are high mannose-type structures while mainly complex- and hybrid-type structures are detected at asparagine 153. *In vitro* studies have shown that the immunological consequences of infection by the CYD dengue viruses 1–4 *versus* the wild type parents are comparable in human monocyte-derived dendritic cells. Our E-protein glycan characterizations of CYD are consistent with those observations from the wild type parents and thus support *in vitro* studies. In addition, these data provide new insights for the role of glycans in the dengue virus–host cell interactions.

© 2015 Elsevier Ltd. All rights reserved.

1. Introduction

Dengue disease affects more than 250 million people each year in inter-tropical areas, causing approximately 25,000 deaths, mainly children [1]. Dengue viruses (DENV) are enveloped flaviviruses transmitted by *Aedes* mosquitoes [2]. During infection, DENV enters target cells *via* specific receptors. Both the identification and the exact role of these receptors remain not completely understood [3]. Recently, cell-surface glycosaminoglycans have been studied [4], TIM and TAM proteins were also identified as possible entry factors [5]. All these molecules might play a role for the DENV entry and could be used as receptors to enter different types of cells [6]. Additionally, several studies described the interaction of DENV with C-type lectins cell-surface like the DC-specific ICAM3-grabbing non-integrin DC-SIGN/CD209 [7]. So far, DC-SIGN is assumed to be the most important DENV co-receptor [8], and a target for antiviral therapy. DENV is able to infect many types of host cells, but some subtypes of human dendritic cells (DCs) are the primary targets of DENV. In this case, the infection is mediated partially by the binding of DENV to DC-SIGN.

The DENV particle is composed of three structural proteins: a capsid (C), a premembrane (prM) and the envelope (E) proteins [9]. These proteins are involved in both the assembly and the maturation of DENV [10]. The E-protein is associated with the prM in immature virions [11]. Through the cellular secretion pathway, the prM-protein is cleaved into M by cellular furin protease, followed with a E-protein conformational rearrangement. The E-protein is the major glycoprotein surface [12], responsible for virus attachment and fusion, and constitutes the primary protective antigen [13]. It is now acknowledged that N-glycosylation of

* Corresponding author: Tel.: +33 4 37 37 97 88; fax: +33 4 37 37 31 49.
E-mail address: jean.dubayle@sanofipasteur.com (J. Dubayle).

http://dx.doi.org/10.1016/j.vaccine.2015.01.047
0264-410X/© 2015 Elsevier Ltd. All rights reserved.

viral proteins plays a central role in virus–host cells receptors and co-receptors interactions [14]. In this respect, characterization of the N-glycosylation state of viral glycoproteins becomes necessary for the understanding of the virus/receptors interaction.

The E-protein contains two potential N-linked glycosylation sites at asparagine residues Asn67 and Asn153. These glycosylation sites are strictly conserved between the different dengue serotypes. The most frequently glycosylation motif observed in the flavivirus E-protein occurs for Asn153 in domain I, which is located near the fusion peptide of the opposite E in the dimeric E conformation of the mature virion [15]. Glycosylation of Asn67 is specific from DENV and located in domain II. The different serotypes and host cell systems described in the literature are known to dramatically influence the presence of glycans and their glycosylation patterns. Furthermore, N-glycosylation characterization of DENV has been reported from lectin interaction studies, exoglycosidase treatment, mutation experiments, combined with cell infection. However, none of these studies investigate the complete glycosylation pattern of DENV.

In this context, some previous studies have demonstrated the presence of N-linked glycans on both sites for all four serotypes [16]. The analysis of the N-linked glycans composition on DENV strongly indicates that the virus has a heterogeneous population of both high-mannose and complex glycans in mammalian cells. On the other hand, E-protein is glycosylated at Asn67 and Asn153 for serotype 1 but only at Asn67 for serotype 2, when DENV is expressed from insect cells [17]. Glycan analysis of a soluble recombinant E-protein from DENV2 expressed in human embryonic kidney cells showed that it bears either complex or hybrid N-linked glycans with 40% sialylated and 25% fucosylated glycoforms [18].

As described above, the presence of N-glycans from the E-protein could directly be related to its ability to interact with receptors. DC-SIGN receptor interacts with mannose and fucose-based oligosaccharides, particularly the Lewis blood group antigen [7]. In dengue virus, DC-SIGN preferentially binds to the terminal mannose residues, and this terminal mannosylation of E-protein is essential for DCs infection [19,20]. Several mutation experiments have shown that N-linked glycosylation at Asn67 is required for virus growth in mammalian cells and important for infectivity [21,22]. Recently, another group revealed that these results were influenced by the strain origin and the nature of the mutation [23]. Furthermore, the structure of an intact lipid-envelope virus DENV2 with the carbohydrate recognition domain of DC-SIGN was obtained [24]. Their cryoelectron microscopy reconstruction gave strong evidence for DC-SIGN binding to N-linked glycans at Asn67 of the two neighboring E-proteins. All these results are consistent and support the key role of the E-protein and glycosylation sites, mediating interaction with DC-SIGN molecules.

The Sanofi Pasteur tetravalent dengue vaccine (CYD dengue vaccine) is composed of four chimeric viruses [25] based on the backbone of the live attenuated yellow fever 17D vaccine, and expressing the major structural antigens prM and E of each dengue serotype. The CYD dengue vaccine candidate has been the subject of an extensive preclinical, clinical and industrial development [26,27]. Large Phase III efficacy studies in Asia and Latin America have recently demonstrated its ability to protect against disease [28,29]. As DENV, the CYD dengue viruses are able to infect human DCs *in vitro*, involving the cell-surface DC-SIGN molecules [30]. The CYD dengue viruses can replicate further in human primary cells such as monocyte-derived dendritic cells, and viremia can be detected *in vivo* after immunization, albeit at low levels [26]. Nevertheless, the first cycle of infection will impact subsequent ones *in vivo* (depending on its initial level and on the identity of target cells), and then the nature of the glycosylation obtained in vero cells has to be considered.

As mentioned above, glycosylation is a critical protein attribute for the ability of CYD dengue viruses to interact with DC-SIGN, which consequently needs further characterization. The glycosylation state of the E-protein from each considered serotype is described in this paper. Since N-glycosylation is dependent on cells subtype and various culture parameters [31], in-depth characterization of N-linked glycans from the E-protein of CYD produced in vero cells is particularly essential. We then considered the glycosylation state of the E-protein from each serotype.

In this work, N-linked oligosaccharides of the E-protein after in-gel deglycosylation have been characterized using mass spectrometry. N-glycosylation profiling of the E-protein was performed using MALDI-TOF, demonstrating that the CYD envelope had a heterogeneous pattern. Furthermore, a detailed study of both Asn67 and Asn153 sites was carried out from glycopeptides. The results show that high mannose glycans are predominant at Asn67 while mainly complex glycans are detected at Asn153.

2. Materials and methods

2.1. Purification of CYD virus particles

ChimeriVax™-DEN1-4 were produced on serum-free vero cells on microcarriers in bioreactor at Sanofi Pasteur (Marcy L'Etoile, France). The viruses were then precipitated on 7% polyethylene glycol-8000, and after 2 h of incubation at 4 °C, the pellets were collected by centrifugation at 16,000 × *g* at 4 °C for 1 h and suspended in 50 mM Tris pH 7.5, 75 mM NaCl, 0.1 mM EDTA. The concentrated virus suspension was loaded onto a 30–50% linear sucrose gradient in the same buffer and centrifuged for 18 h at 160,000 × *g* at 4 °C in a Beckman SW32 rotor. Sixty fractions of 500 μl were collected and the presence of virus was detected in each fraction by qRT-PCR targeted yellow fever 17D-NS5 gene [32]. Virions present in the fractions with the highest titers were pooled and diafiltrated twice on Amicon 100 kDa to eliminate sucrose and replace by buffer 50 mM Tris pH 7.5, 75 mM NaCl, 0.1 mM EDTA. Purified CYD viruses were stored at −80 °C.

2.2. Protein identification and Isolation of E protein from CYD virus particules

The proteins from purified CYD virus particules were separated using SDS-PAGE after protein reduction and alkylation. Gels were stained with GelCode® blue stain reagent. Analytical gel was done with 5 μg protein. All detected bands were excised and identifications were performed. Tryptic digestion was performed using DigestPro MS robot (Intavis AG Bioanalytical Instruments, Germany). Excised gel bands were washed alternatively with 50 mM ammonium bicarbonate, pH 8 and acetonitrile. Proteins were then reduced with 10 mM DTT and alkylated with 55 mM iodoacetamide and then enzymatically digested with trypsin at 0.01 mg/ml diluted in 25 mM ammonium bicarbonate (Promega, USA). Samples were incubated at 37 °C during 4 h. Digestion was stopped by the addition of trifluoroacetic acid (TFA) at a final concentration 0.1% (v/v) and the resulting peptides were collected. The samples were then deposited onto a matrix layer of saturated α-cyano-4-hydroxycinnamic acid solution in acetone and TFA 0.1% (v/v), as described [33]. Analyses were performed on an Ultraflextreme MALDI-TOF mass spectrometer in reflectron positive mode (Bruker Daltonics, Billerica, MA). External calibration was done in each case using peptide calibrants (Bruker Daltonics, reference 222570). Mass spectra were acquired using sets of instrument parameters over 800–4000 *m*/*z*. Monoisotopic peptide masses determined by MALDI-TOF were submitted to the MASCOT

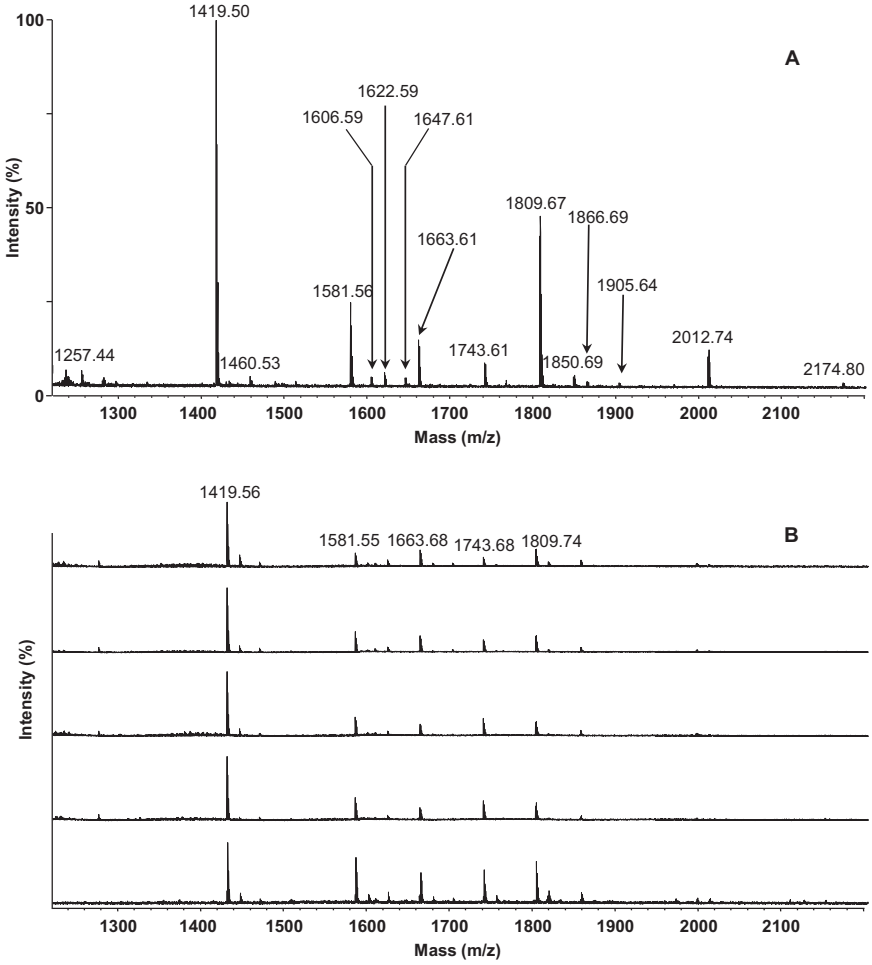

Fig. 1. (A) N-glycans present on CYD-3 E-protein. (B) Batch to batch comparison of N-glycans present on CYD-2 E-protein. The N-glycans from the E-protein were released by in-gel PNGase F deglycosylation, micropurified and measured by MALDI-TOF positive mode using 2,5-dihydroxybenzoic acid matrix. Detected ions are singly charged sodium adducts and monoisotopic masses are shown above the peak. For assignments of glycans see Table 1.

program (Matrix Science Ltd.). The recorded peptide masses were then matched with the masses resulting from theoretical digests of the protein sequences currently present in the Uniprot or MSDB databases. A peptide tolerance of 50 ppm was permitted and one trypsin miss cleavage was considered.

For glycosylation studies, 15 μg of protein was loaded. Detected bands of E-protein were cut and in-gel digested by endoglycosidase peptide-N4-(N-acetyl-β-D-glucosaminyl) asparagine amidase F (PNGase F) and/or by trypsin or trypsin/Glu C.

2.3. In-gel deglycosylation of glycoproteins with the endoglycosidase peptide-N4-(N-acetyl-β-D-glucosaminyl) asparagine amidase F

A modified version of the protocols reported by [34,35] was used. Excised gel bands were extensively rinsed with de-ionized water before equilibration with 20 mM sodium carbonate, pH 7. In order to remove sodium dodecyl sulfate, the gel was alternately washed twice with 100% acetonitrile and sodium carbonate buffer.

Table 1
Proposed carbohydrate composition of N-glycans released from the E-protein observed by MALDI-TOF in Figs. 1 and 2.

m/z [M+Na$^+$] experimental	m/z [M+Na$^+$] calculated	N-glycans composition	N-glycans type
1257.448	1257.423	$Man_5GlcNAc_2$	High mannose
1419.506	1419.476	$Man_6GlcNAc_2$	High mannose
1581.556	1581.529	$Man_7GlcNAc_2$	High mannose
1743.609	1743.582	$Man_8GlcNAc_2$	High mannose
1905.643	1905.634	$Man_9GlcNAc_2$	High mannose
1460.536	1460.503	$GlcNAc_1Man_5GlcNAc_2$	Hybrid
1606.585	1606.560	$GlcNAc_1Man_5GlcNAc_2Fuc_1$	Hybrid
1622.588	1622.555	$Gal_1GlcNAc_1Man_5GlcNAc_2$	Hybrid
1647.614	1647.587	$Gal_1GlcNAc_2Man_3GlcNAc_2Fuc_1$	Complex
1663.608	1663.582	$Gal_2GlcNAc_2Man_3GlcNAc_2$	Complex
1809.667	1809.640	$Gal_2GlcNAc_2Man_3GlcNAc_2Fuc_1$	Complex
1850.693	1850.666	$Gal_1GlcNAc_3Man_3GlcNAc_2Fuc_1$	Complex
1866.688	1866.661	$Gal_2GlcNAc_3Man_3GlcNAc_2$	Complex
2012.744	2012.719	$Gal_2GlcNAc_3Man_3GlcNAc_2Fuc_1$	Complex
2174.796	2174.772	$Gal_3GlcNAc_3Man_3GlcNAc_2Fuc_1$	Complex

After a brief exposure to vaccum, the gel was rehydrated with 5 Sigma unit of PNGase F in carbonate buffer and incubated 16 h at 37 °C. Released N-glycans were eluted from the gels by several washes with water under sonication, subsequently pooled and reduced to a low volume for MALDI-TOF analysis. As a control, the same protocol was performed from excised gel bands but with addition of carbonate buffer instead of PNGase F. This control sample was used to identify the experimental false positives deamidated Asn residues [36].

2.4. In-gel proteolysis of glycoproteins

Enzymatic digestion was done from excised gel bands following a modified version of the protocol reported by [34,37]. Excised gel bands were extensively rinsed with de-ionized water before equilibration with 25 mM ammonium bicarbonate pH 8, 50% acetonitrile. In order to remove sodium dodecyl sulfate, the gel was alternately washed twice with 100% acetonitrile and 25 mM ammonium bicarbonate, 50% acetonitrile during 15 min. Then, gel bands were shrunk by replacement of buffer with 100% acetonitrile, and exposed briefly to vacuum. The gel bands were swollen in 25 mM ammonium bicarbonate containing 12.5 μg/ml of trypsin (Promega, USA) in an ice-cold bath during 45 min. Then the supernatant was removed and replaced with digestion buffer without trypsin to keep the gel pieces wet. Cleavage proceeded at 37 °C for 16 h for trypsin digestion. For the double digest, trypsin digestion was incubated during 4 h at 37 °C, and 2 μl of endoproteinase GluC (Roche, Germany) at 1 mg/ml was added and then incubated at 25 °C during 16 h. Peptides were extracted alternatively with 30% acetonitrile, TFA 0.1% and 80% acetonitrile, TFA 0.1% during 10 min with sonication. The supernatant and extracts were combined and evaporated to 5 μl, then diluted with TFA 0.05% before injection.

2.5. Matrix-assisted laser desorption/ionization time-of-flight mass spectrometries (MALDI-TOF-MS) of N-glycans

MALDI-TOF spectra were recorded on a Bruker Ultraflextreme in reflectron positive mode for neutral glycans and in negative mode for acidic glycans. 2,5-Dihydroxybenzoic acid was used as matrix and the neutral glycans were detected as singly charged sodium adducts [38]. 6-Aza-2-thiothymine was used as matrix for acidic glycans [39] which were detected as negatively singly charged $[M-H]^-$ species. N-glycans were micropurified by graphite phase or dowex cation exchange resin prior MALDI-TOF analysis using dried droplet method.

2.6. Nanochromatography coupled with electrospray mass spectrometry (NanoLC–ESI-MS/MS) of glycopeptides

The nano-LC/ESI-MS/MS experiments were performed using an Ultimate HPLC system (Dionex GmbH, Germany) equipped with a 150 mm × 0.075 mm PepMap RP C18 column and a 5 mm × 0.3 mm preconcentration RP C18 column, which were online coupled to a Bruker Maxis Q-TOF mass spectrometer or an ion trap HCT. The mobile phase consisted of a 0.1% formic acid in 2% acetonitrile/98% water (A) and 0.08% formic acid in 80% acetonitrile/20% water (B). The sample was diluted with 0.1% TFA and injected. A linear gradient from 2 to 35.5% B in 90 min was used at flow rate of 250 nl/min. The mass spectrometer was operated in the positive ion mode in an *m/z* range of 300–1500 *m/z*. Peptides were fragmented using autoMS/MS over the same scan range with active exclusion for 1 min and with three precursor ions being selected per cycle. Detection of glycopeptides was based on the MS/MS signal of characteristic ions 366, 528 and 690 *m/z* from fragmented

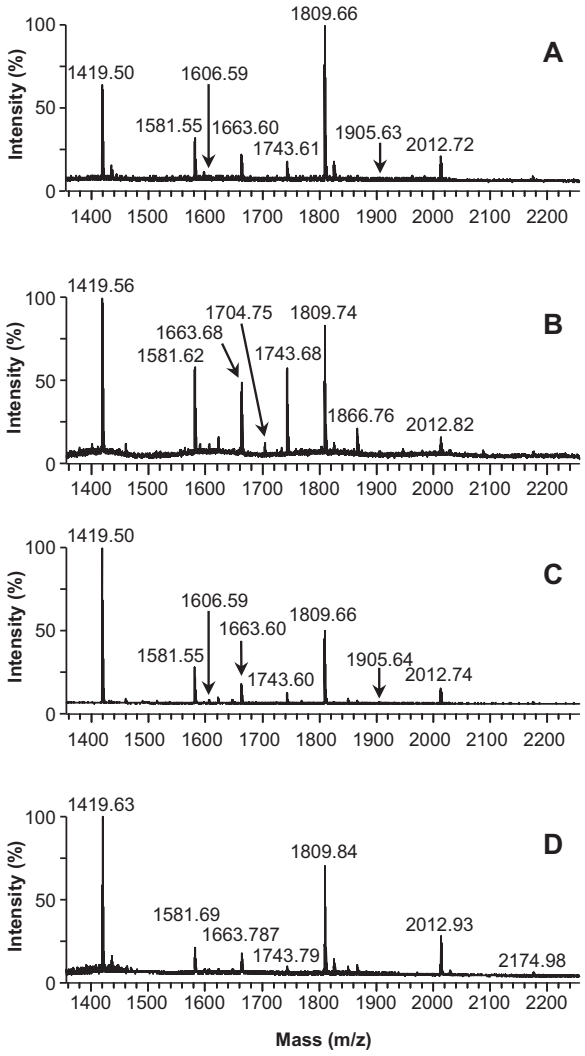

Fig. 2. N-glycans present on the E-protein from CYD-1 (A), CYD-2 (B), CYD-3 (C) and CYD-4 (D). The N-glycans from the E-protein were released by in-gel PNGase F deglycosylation, micropurified and measured by MALDI-TOF positive mode using 2,5-dihydroxybenzoic acid matrix. Detected ions are singly charged sodium adducts and monoisotopic masses are shown above the peak. For assignments of glycans see Table 1.

glycopeptides. Data were manually interpreted and identification was based on MS and MS/MS measurements. Putative structures of N-glycans were deduced from composition based on accurate mass measurements. Data from deglycosylated peptides resulting from in gel deglycoyslation and proteolysis were submitted to the MASCOT program. Identification of peptides containing the N-glycosylation sites was performed by accurate mass measurements and MS/MS analysis.

2.7. Sialic acids assay

Sialic acids were released from CYD-2 glycoproteins after 2 h acetic acid 1% (v/v) hydrolysis at 80 °C [40]. High performance anion exchange chromatographic separation was performed on a Dionex ICS 3000 system (Sunnyvale, CA, USA). A carbopac PA10 column with guard column was used and sialic acids were separated with an isocratic 90 mM sodium acetate–75 mM sodium hydroxide and detected by pulsed amperometric detection. Samples were quantified against standard sialic acids reference.

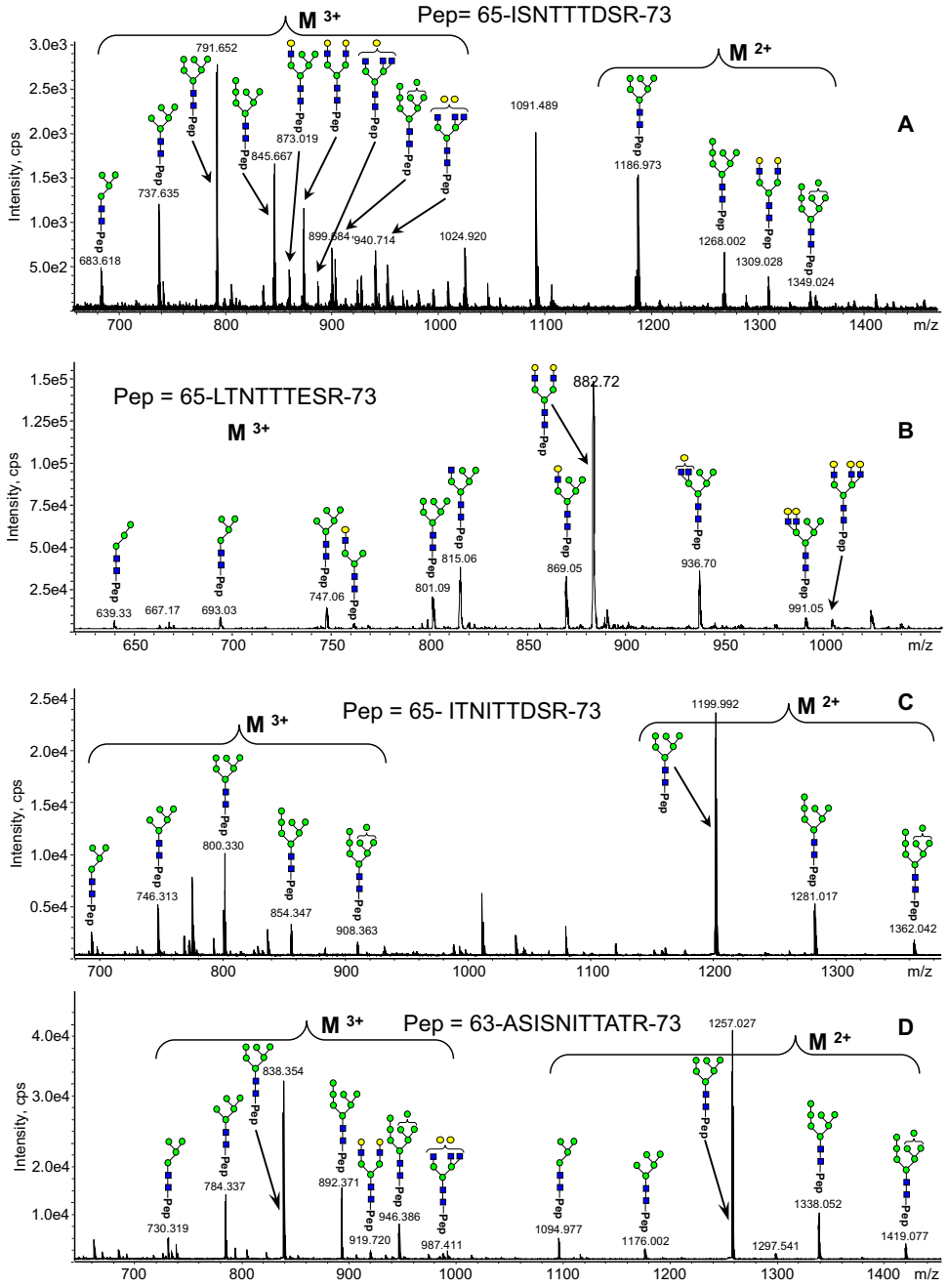

Fig. 3. NanoLC–MS/MS experiments from glycopeptides Asn67 site derived from the E-protein digest CYD-1 (A), CYD-2 (B), CYD-3 (C), and CYD-4 (D). Several glycoforms are identified based on accurate mass measurements and their MS/MS spectra. One possible structure of the glycan species is represented from mass measurements. The compounds are represented by the symbols (blue rectangle, GlcNAc; green circle, mannose; red triangle, fucose; yellow circle, galactose; red diamond, sialic acid). (For interpretation of the references to color in this figure legend, the reader is referred to the web version of this article.)

3. Results

3.1. SDS-PAGE analysis of the E-protein

Based on mass spectrometry data derived from trypsin digestion, we found out that the major protein from each serotype is the E-protein, which is the major immunogenic target of the CYD dengue vaccine. N-glycans resulting from in-gel deglycosylation of bands corresponding to the E-protein were analyzed first using MALDI-TOF.

3.2. N-glycosylation profiling of the E-protein

N-glycans profiling from the E-protein CYD-3 (Fig. 1A) showed a family of high mannose glycans comprised between 5 and 9 mannose residues. The predominant ion peak at *m*/*z* 1419.506 corresponds to $Hex_6HexNAc_2$ which can be assigned to $Man_6GlcNAc_2$. Several other complex or hybrid N-glycans are detected too (Table 1). Among them, the predominant ion peak at *m*/*z* 1809.667 corresponds to $HexNAc_2Hex_5HexNAc_2Fuc_1$ that is most likely a complex N-glycan. Minor ion peaks at *m*/*z* 1460.536, *m*/*z*

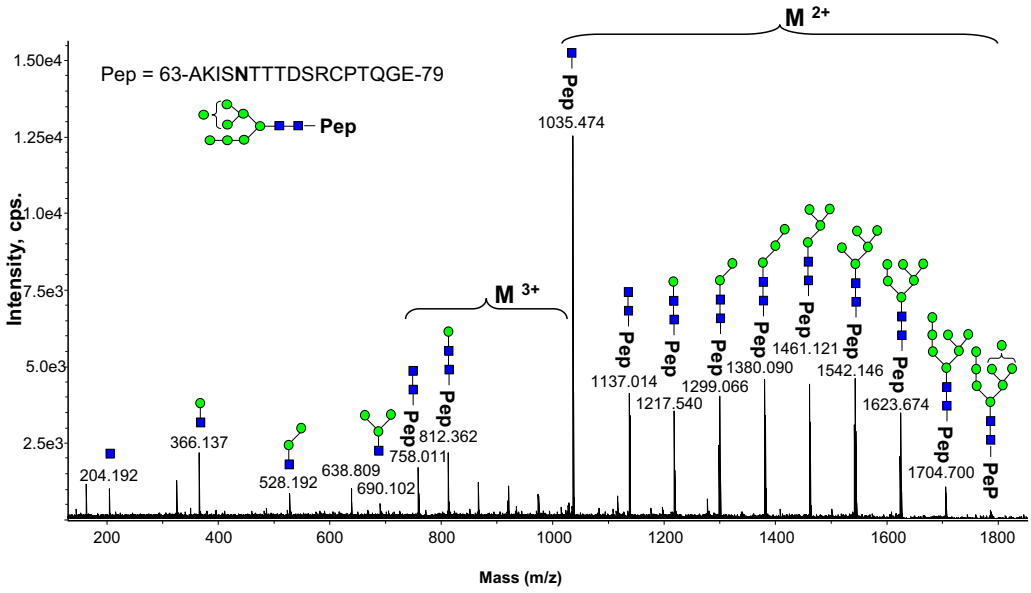

Fig. 4. Positive ion CID MS/MS spectra of the parent ion at *m/z* 1190.15 from CYD-1 E-protein, corresponding to the glycopeptide containing the site Asn67. The identities of the fragment are indicated above the fragment ion masses. Same fragments are identified from triply (3+) or doubly (2+) charged species and correspond to N-glycan composition $Man_8GlcNAc_2$. The compounds are represented by the symbols as in Fig. 3 (blue rectangle, GlcNAc; green circle, mannose; red triangle, fucose; yellow circle, galactose; red diamond, sialic acid). (For interpretation of the references to color in this figure legend, the reader is referred to the web version of this article.)

1606.585 and *m/z* 1622.588 correspond to $HexNAc_1Hex_5HexNAc_2$, $HexNAc_1Hex_5HexNAc_2Fuc_1$ and $HexNAc_1Hex_6HexNAc_2$ respectively, which are hybrid type N-glycans. Most of the detected N-glycans are biantennary structures while some minor peaks are triantennary structures. The comparison of several batches from all serotypes described a similar picture. As observed in Fig. 1B, similar N-glycosylation profile were obtained from five different CYD-2 batches, and differs only in the relative peaks intensities. In a similar way, N-glycan profiling from the four serotypes exhibits intensity differences for the major peaks (Fig. 2). One can imagine that this last observation could be related to the analysis of underivatized glycans and/or significant variability of MALDI-TOF signal as it has been widely reported in the literature.

Comparison of N-glycan profiling from the four serotypes shows the same pattern of N-glycosylation comprised high mannose, complex and hybrid glycans (Fig. 2). The results showed high similarity for the number of N-glycans identified between each serotype. Some high mannose type glycans like $Man_5GlcNAc_2$ at *m/z* 1257.45, $Man_9GlcNAc_2$ at *m/z* 1905.64 and hybrid type $GlcNAc_1Man_5GlcNAc_2Fuc_1$ at *m/z* 1606.58 are only detected for CYD-1 (Fig. 2A) and CYD-3 (Figs. 1A and 2C) serotypes. The N-glycan $Gal_1GlcNAc_3Man_3GlcNAc_2$ at *m/z* 1704.75 is detected only for CYD-2 serotype.

Sialylated complex fucosylated and non-fucosylated N-glycans from CYD-1 and CYD-3 serotypes containing only one N-acetylneuraminic acid (NeuAc) residue, at *m/z* 1930.71, *m/z* 2076.77, and *m/z* 2441.90 (Supplementary Fig. 1) were also detected. These peaks could correspond to $NeuAc_1Gal_2GlcNAc_2Man_3GlcNAc_2$, $NeuAc_1Gal_2GlcNAc_2Man_3GlcNAc_2Fuc_1$ and $NeuAc_1Gal_3GlcNAc_3Man_3GlcNAc_2Fuc_1$ N-glycans respectively. In addition, the ion peak at *m/z* 2092.767 seems to be a hybrid N-glycan $NeuAc_1Gal_2GlcNAc_2Man_4GlcNAc_2$. Based on their composition, these N-glycans are bi or triantennary structures. MALDI-TOF analysis of underivatized sialylated N-glycans could lead to the loss of sialic acids when 2,5-dihydroxybenzoic acid matrix is used. However, many of these fragmentation problems using MALDI-TOF can be overcome by a suitable choice of matrix. In our experimental conditions, the use of 6-aza-2-thiothymine matrix instead of 2,5-dihydroxybenzoic acid increases significantly the detection of sialylated glycans [38,39]. However, we were unable to detect sialylated glycans from CYD-2 and CYD-4 serotype suggesting that the amount of these N-glycans is below the limit of quantification. Analysis by HPAEC confirmed the presence of N-acetylneuraminic acid from CYD-2 at a ratio below 0.03 μg per mg of proteins and no N-glycolylneuraminic acid could be detected (data not shown).

3.3. Site-specific characterization of glycopeptides from E-protein

Identification of glycosylation site was based on the comparison of proteolytic peptides obtained with and without PNGase F protein deglycosylation as a control. For each serotype, peptides containing Asn67 and Asn153, the two potential glycosylation sites, were not detected in their non-glycosylated form in the control samples without PNGase F treatment. On the other hand, peptides containing both Asn67 and Asn153 glycosylation sites were detected after PNGase F deglycosylation, suggesting that both non-glycosylated peptides are eluted from the column. Accurate mass measurements and MS/MS analysis of the peptides confirmed the conversion of asparagine to aspartic acid residues following protein deglycosylation using PNGase F (mass shift of +0.98 Da).

3.4. Glycopeptides derived from Asn67 of E-protein

The main glycopeptides detected containing Asn67, have N-linked high mannose composed of 4–8 mannose residues, for serotype CYD-1, CYD-3 and CYD-4 (Fig. 3). N-glycan compositions are deduced from accurate mass measurements and MS/MS data. Fig. 4 shows an example of a MS/MS spectrum for the triply charged precursor (*m/z* 1190.15), which was identified as the $Man_8GlcNAc_2$ glycoform at the Asn67 site. The MS/MS spectrum provides direct evidence for the high mannose-type glycosylation linked to Asn67 site. MS/MS data were obtained for each serotype and confirmed the presence of various glycoforms at this position Asn67 (Supplementary Table 1).

For CYD-2, high mannose linked to Asn67 glycopeptides showed less intense signal than complex or hybrid N-linked glycans (Fig. 3B). Surprisingly, the only glycan family detected for CYD-3 Asn67 site is high mannose as shown in Fig. 3C. The other serotypes showed complex and hybrid glycopeptides from Asn67

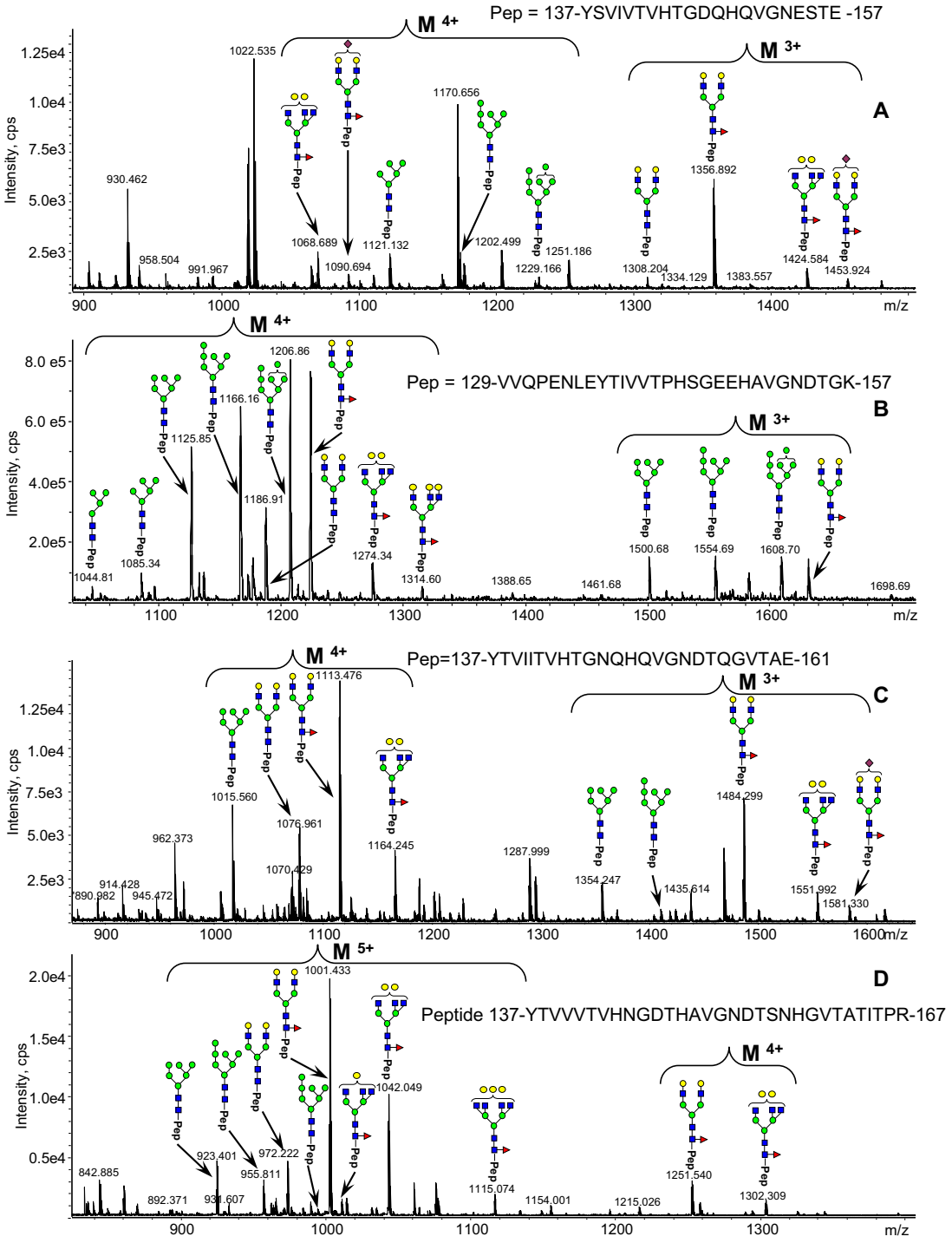

Fig. 5. NanoLC–MS/MS experiments from glycopeptides Asn153 site derived from the E-protein digest CYD-1 (A), CYD-2 (B), CYD-3 (C), and CYD-4 (D). Several glycoforms are identified based on accurate mass measurements and their MS/MS spectra. One possible structure of the glycan species is represented from mass measurements. The compounds are represented by the symbols as in Fig. 3 (blue rectangle, GlcNAc; green circle, mannose; red triangle, fucose; yellow circle, galactose; red diamond, sialic acid). (For interpretation of the references to color in this figure legend, the reader is referred to the web version of this article.)

(Supplementary Table 1). These are bi or tri antennary glycans without fucosylation. Complex sialylated glycopeptides derived from Asn67 are detected from CYD-1 and CYD-2 at very low amounts.

3.5. Glycopeptides derived from Asn153 of E-protein

Major glycopeptides detected for Asn153 for CYD-1, CYD-3 and CYD-4 serotype contain complex or hybrid linked glycans with fucosylation and bi-antennary structure (Fig. 5). For the CYD-2 serotype, major glycopeptides for Asn153 are high mannose linked glycan $Man_8GlcNAc_2$ (m/z 1206.86) and a complex-type glycan $Gal_2GlcNAc_2Man_3GlcNAc_2Fuc_1$ (m/z 1230). High mannose linked glycans are detected from all serotypes at Asn153 (Supplementary Table 2) and consist of 6–8 mannose residues, except for CYD-2 E-protein which has 4–8 mannose residues (Fig. 5B). Complex sialylated glycopeptides are also detected at this position at very low intensity. Surprisingly, fucosylated glycopeptides were specific for the Asn153 site and not detected for Asn67.

4. Discussion

In this study, we compared the glycosylation pattern and the site specific N-glycosylation of the E-protein from four serotypes of the CYD dengue vaccine candidate. The glycosylation pattern was elucidated using MALDI-TOF. The characterization of site specific N-glycosylation was assessed by nanoLC–ESI-MS/MS. Previous studies related to N-glycosylation of the DENV were done using lectin reactivity, virus mutation, or exoglycosidase treatment. So far, no reports of the specific N-glycosylation pattern of the E-protein using mass spectrometry are mentioned in the literature. Here, we used a combination of mass spectrometry methods to biochemically characterized the N-glycosylation of the E-protein from the dengue vaccine candidates produced in vero cells.

Analysis of the N-glycan profile of the E-protein by MALDI-TOF demonstrates a high heterogeneity, with 15 neutral N-glycans and 4 sialylated N-glycans. The presence of high mannose, complex and hybrid glycans are in agreement with the glycosylation profiles of glycoproteins produced in vero cells. The main peak corresponds to high mannose glycan: $Man_6GlcNAc_2$, as described in previous studies realized on the wild-type dengue viruses expressed on mosquito cells [17]. In addition, we detected different complex and hybrid glycans as previously characterized using the lectin reactivity experiments on the E-protein expressed in vero cells [20]. The second more intense peak corresponds probably to a complex fucosylated glycan: $Gal_2GlcNAc_2Man_3GlcNAc_2Fuc_1$. This glycan was previously detected using LC and sequential digestion of the soluble recombinant E-protein expressed in mammalian cells [18]. On the other hand, we found a very low number of sialylated glycans. Our data provide a complete glycosylation pattern of the E-protein that was not assessed previously. The glycan composition is in agreement with the ability of the four CYD dengue viruses to interact with DC-SIGN as described in the literature [7]. The same global N-glycosylation pattern is observed for the four serotypes, suggesting that glycans interactions with DCs are similar for the different dengue virions. These interactions ensure a proper activation of the DCs by CYD vaccine, as observed in human monocyte-derived dendritic cells [30,41].

Identification of the N-glycosylation sites and site-specific glycan micro-heterogeneity were characterized using nanoLC–ESI-MS/MS. Our data show that both sites, Asn67 and Asn153, are fully glycosylated, because we did not detect non-glycosylated peptides. We identified a total of 29 different neutral glycoforms and 6 sialylated glycoforms of the E-protein. As expected, we were able to detect more glycoforms using nanoLC–ESI-MS/MS than MALDI-TOF.

Our data demonstrate that the most abundant glycoforms at each site of the E-protein are different. The main glycoforms at Asn67 residue are high mannose-type structures, and correspond to a $Man_6GlcNAc_2$ glycoform. On the other hand, the most abundant glycoforms at Asn153 residue are complex-type structures, and corresponds most likely to a $Gal_2GlcNAc_2Man_3GlcNAc_2Fuc_1$ glycoform. These two glycans are the ones predominantly detected using MALDI-TOF. Surprisingly, fucosylated glycopeptides are found at Asn153 but not at Asn67.

Minor differences in the relative distribution of glycoforms between serotypes can be observed. These discrepancies may result from method sensitivity limitation, indicating the importance of using a complementary approach to fully determine the glycosylation state of the E-protein. Moreover, the determination of the relative abundance of the glycoforms at each specific glycosylation site is very important to elucidate the full glycosylation pattern of the E-protein. Further studies should be undertaken in order to determine accurately the relative abundance of each glycoform at both sites, using several vaccine batches for each serotype.

In summary, our current work provides information on the site-specific N-glycosylation of the E-protein from CYD-1 to 4. The composition of the N-glycans identified in this study is in agreement with the structures described for the wild-type dengue virus in the literature. These data demonstrate that both Asn67 and Asn153 are glycosylated, and that the main glycoform detected is able to interact with DC-SIGN receptor, known to be the most important DENV receptor. *In vitro* studies have shown that the immunological consequences of CYD dengue viruses 1–4 infection *versus* the wild type parents are comparable in human monocyte-derived dendritic cells. The E-protein glycan characterization of CYD is consistent with those from the wild-type parents and thus support *in vitro* studies [30,41]. Finally, our mass spectrometry data bring new insights into the characterization of the role of N-glycans in the dengue–host cell interaction. The same analysis of the glycans composition can be broadly applicable to different virus in order to establish a more general function of glycans in the host infection.

Acknowledgments

The authors would like to warmly acknowledge Fabienne Barrière, Manon Fradin, Catherine Louis-Alonso, Vanessa Buosi, Grenville Marsh, Jo-Ann West, Marie-Pauline Ayroles, Paul Commander, Véronique Barban, Jean Lang, Nicholas Jackson, and all Sanofi Pasteur team members.

Conflict of interest: The authors are all employees of Sanofi Pasteur, however they declare no conflict of interest.

Appendix A. Supplementary data

Supplementary data associated with this article can be found, in the online version, at http://dx.doi.org/10.1016/j.vaccine.2015.01.047.

References

[1] Simmons CP, Farrar JJ, Nguyen v, Wills B. Dengue. N Engl J Med 2012;366(15):1423–32.
[2] Mukhopadhyay S, Kuhn RJ, Rossmann MG. A structural perspective of the flavivirus life cycle. Nat Rev Microbiol 2005;3(1):13–22.
[3] Hidari KI, Suzuki T. Dengue virus receptor. Trop Med Health 2011;39(4 (Suppl.)):37–43.
[4] Watterson D, Kobe B, Young PR. Residues in domain III of the dengue virus envelope glycoprotein involved in cell-surface glycosaminoglycan binding. J Gen Virol 2012;93(Pt 1):72–82.
[5] Meertens L, Carnec X, Lecoin MP, Ramdasi R, Guivel-Benhassine F, Lew E, et al. The TIM and TAM families of phosphatidylserine receptors mediate dengue virus entry. Cell Host Microbe 2012;12(4):544–57.
[6] Fang S, Wu Y, Wu N, Zhang J, An J. Recent advances in DENV receptors. Sci World J 2013;2013.
[7] Svajger U, Anderluh M, Jeras M, Obermajer N. C-type lectin DC-SIGN: an adhesion, signalling and antigen-uptake molecule that guides dendritic cells in immunity. Cell Signal 2010;22(10):1397–405.
[8] Alen MM, Schols D. Dengue virus entry as target for antiviral therapy. J Trop Med 2012;2012.
[9] Kuhn RJ, Zhang W, Rossmann MG, Pletnev SV, Corver J, Lenches E, et al. Structure of dengue virus: implications for flavivirus organization, maturation, and fusion. Cell 2002;108(5):717–25.
[10] Perera R, Kuhn RJ. Structural proteomics of dengue virus. Curr Opin Microbiol 2008;11(4):369–77.
[11] Zhang Y, Corver J, Chipman PR, Zhang W, Pletnev SV, Sedlak D, et al. Structures of immature flavivirus particles. EMBO J 2003;22(11):2604–13.
[12] Smith GW, Wright PJ. Synthesis of proteins and glycoproteins in dengue type 2 virus-infected vero and *Aedes albopictus* cells. J Gen Virol 1985;66(Pt 3):559–71.
[13] Heinz FX, Stiasny K. Flaviviruses and flavivirus vaccines. Vaccine 2012;30(29):4301–6.
[14] Backovic M, Rey F. Virus entry: old viruses, new receptors. Curr Opin Virol 2012;2:4–13.
[15] Modis Y, Ogata S, Clements D, Harrison SC. A ligand-binding pocket in the dengue virus envelope glycoprotein. Proc Natl Acad Sci USA 2003;100(12):6986–91.
[16] Hacker K, White L, de Silva AM. N-linked glycans on dengue viruses grown in mammalian and insect cells. J Gen Virol 2009;90(Pt 9):2097–106.

[17] Johnson AJ, Guirakhoo F, Roehrig JT. The envelope glycoproteins of dengue 1 and dengue 2 viruses grown in mosquito cells differ in their utilization of potential glycosylation sites. Virology 1994;203(2):241–9.
[18] Miller JL, de Wet BJ, Martinez-Pomares L, Radcliffe CM, Dwek RA, Rudd PM, et al. The mannose receptor mediates dengue virus infection of macrophages. PLoS Pathog 2008;4(2):e17.
[19] Alen MM, Dallmeier K, Balzarini J, Neyts J, Schols D. Crucial role of the N-glycans on the viral E-envelope glycoprotein in DC-SIGN-mediated dengue virus infection. Antivir Res 2012;96(3):280–7.
[20] Dejnirattisai W, Webb AI, Chan V, Jumnainsong A, Davidson A, Mongkolsapaya J, et al. Lectin switching during dengue virus infection. J Infect Dis 2011;203(12):1775–83.
[21] Bryant JE, Calvert AE, Mesesan K, Crabtree MB, Volpe KE, Silengo S, et al. Glycosylation of the dengue 2 virus E protein at N67 is critical for virus growth in vitro but not for growth in intrathoracically inoculated *Aedes aegypti* mosquitoes. Virology 2007;366(2):415–23.
[22] Mondotte JA, Lozach PY, Amara A, Gamarnik AV. Essential role of dengue virus envelope protein N glycosylation at asparagine-67 during viral propagation. J Virol 2007;81(13):7136–48.
[23] Lee E, Leang SK, Davidson A, Lobigs M. Both E protein glycans adversely affect dengue virus infectivity but are beneficial for virion release. J Virol 2010;84(10):5171–80.
[24] Pokidysheva E, Zhang Y, Battisti AJ, Bator-Kelly CM, Chipman PR, Xiao C, et al. Cryo-EM reconstruction of dengue virus in complex with the carbohydrate recognition domain of DC-SIGN. Cell 2006;124(3):485–93.
[25] Guy B, Saville M, Lang J. Development of Sanofi Pasteur tetravalent dengue vaccine. Hum Vaccine 2010;6(9):696–705.
[26] Guy B, Barrere B, Malinowski C, Saville M, Teyssou R, Lang J. From research to phase III: preclinical, industrial and clinical development of the Sanofi Pasteur tetravalent dengue vaccine. Vaccine 2011;29(42):7229–41.
[27] Sabchareon A, Wallace D, Sirivichayakul C, Limkittikul K, Chanthavanich P, Suvannadabba S, et al. Protective efficacy of the recombinant, live-attenuated, CYD tetravalent dengue vaccine in Thai schoolchildren: a randomised, controlled phase 2b trial. Lancet 2012;380(9853):1559–67.
[28] Capeding MR, Ngoc HT, Sri Rezeki SH, Hussain Imam HJMI, Tawee C, Mary NC, et al. Clinical efficacy and safety of a novel tetravalent dengue vaccine in healthy children in Asia: a phase 3, randomised, observer-masked, placebo-controlled trial. Lancet 2014;384:1358–65, http://dx.doi.org/10.1016/S0140-6736(14)61060-6.
[29] Villar L, Dayan GH, Arredondo-García JL, Rivera DM, Cunha R, Deseda C, et al. Efficacy of a tetravalent dengue vaccine in children in latin America. N Engl J Med 2015;372(2):113–23.
[30] Deauvieau F, Sanchez V, Balas C, Kennel A, DE Montfort A, Lang J, et al. Innate immune responses in human dendritic cells upon infection by chimeric yellow-fever dengue vaccine serotypes 1–4. Am J Trop Med Hyg 2007;76(1):144–54.
[31] Hossler P, Khattak SF, Li ZJ. Optimal and consistent protein glycosylation in mammalian cell culture. Glycobiology 2009;19(9):936–49.
[32] Mantel N, Aguirre M, Gulia S, Girerd-Chambaz Y, Colombani S, Moste C, et al. Standardized quantitative RT-PCR assays for quantitation of yellow fever and chimeric yellow fever–dengue vaccines. J Virol Methods 2008;151(1):40–6.
[33] Gobom J, Schuerenberg M, Mueller M, Theiss D, Lehrach H, Nordhoff E. Alpha-cyano-4-hydroxycinnamic acid affinity sample preparation. A protocol for MALDI-MS peptide analysis in proteomics. Anal Chem 2001;73:434–8.
[34] Kuster B, Wheeler SF, Hunter AP, Dwek RA, Harvey DJ. Sequencing of N-linked oligosaccharides directly from protein gels: in-gel deglycosylation followed by matrix-assisted laser desorption/ionization mass spectrometry and normal-phase high-performance liquid chromatography. Anal Biochem 1997;250(1):82–101.
[35] Sagi D, Kienz P, Denecke J, Marquardt T, Peter-Katalinic J. Glycoproteomics of N-glycosylation by in-gel deglycosylation and matrix-assisted laser desorption/ionisation-time of flight mass spectrometry mapping: application to congenital disorders of glycosylation. Proteomics 2005;5(10):2689–701.
[36] Parker BL, Palmisano G, Edwards AV, White MY, Engholm-Keller K, Lee A, et al. Quantitative N-linked glycoproteomics of myocardial ischemia and reperfusion injury reveals early remodeling in the extracellular environment. Mol Cell Proteomics 2011;10(8). M110.006833.
[37] Shevchenko A, Wilm M, Vorm O, Mann M. Mass spectrometric sequencing of proteins silver-stained polyacrylamide gels. Anal Chem 1996;68(5):850–8.
[38] Harvey DJ. Matrix-assisted laser desorption/ionization mass spectrometry of carbohydrates. Mass Spectrom Rev 1999;18(6):349–450.
[39] Papac DI, Wong A, Jones AJS. Analysis of acidic oligosaccharides and glycopeptides by matrix-assisted laser desorption/ionization time-of-flight mass spectrometry. Anal Chem 1996;68:3215–23.
[40] Rohrer JS, Thayer J, Weitzhandler M, Avdalovic N. Analysis of the N-acetylneuraminic acid and N-glycolylneuraminic acid contents of glycoproteins by high-pH anion-exchange chromatography with pulsed amperometric detection. Glycobiology 1998;8(1):35–43.
[41] Balas C, Kennel A, Deauvieau F, Sodoyer R, Arnaud-Barbe N, Lang J, et al. Different innate signatures induced in human monocyte-derived dendritic cells by wild-type dengue 3 virus, attenuated but reactogenic dengue 3 vaccine virus, or attenuated nonreactogenic dengue 1–4 vaccine virus strains. J Infect Dis 2011;203:103–8.